IEEE Access
Multidisciplinary | Rapid Review | Open Access Journal

Received January 29, 2022, accepted February 10, 2022, date of publication February 15, 2022, date of current version February 28, 2022.

Digital Object Identifier 10.1109/ACCESS.2022.3151804

Real-Time Control of Active Catheter Signals for Better Visual Profiling During Cardiovascular Interventions Under MRI Guidance

ALI C. ÖZEN[1,2], (Senior Member, IEEE), THOMAS LOTTNER[1], (Member, IEEE), SIMON REISS[1], TIMO HEIDT[2], CONSTANTIN VON ZUR MÜHLEN[2], AND MICHAEL BOCK[1]

[1]Department of Radiology, Medical Physics, Medical Center University of Freiburg, Faculty of Medicine, University of Freiburg, 79106 Freiburg, Germany
[2]Department of Cardiology and Angiology I, University Heart Center, Medical Center University of Freiburg, Faculty of Medicine, University of Freiburg, 79106 Freiburg, Germany

Corresponding author: Ali C. Özen (ali.oezen@uniklinik-freiburg.de)

This work was supported by the Deutsche Forschungsgemeinschaft (DFG) under Grant BO3025/2-2 and Grant SFB1425. The work of Timo Heidt, Constantin Von Zur Mühlen, and Michael Bock was supported in part by the Collaborative Research Consortium (CRC) under Grant SFB1425.

This work involved human subjects or animals in its research. Approval of all ethical and experimental procedures and protocols was granted by the Local Ethics Committee of Freiburg University and the Regional Council of Freiburg, Baden-Wuerttemberg, Germany, under Approval Nos. G-15/156, G-16/78, G-19/70, and G-21/008. Experiments were conducted in accordance with FELASA, GV-SOLAS guidelines for animal welfare and reported in accordance with ARRIVE guidelines.

ABSTRACT In MR-guided interventional procedures, RF coils can be attached to the instruments to provide a positive MR signal for device tracking. The signal from these coils can vary strongly over the procedure and mask the surrounding anatomy. The purpose of this study is to introduce and demonstrate a low-cost, vendor- and device-independent interface circuit that allows the interventionalist to adjust the active device signal intensity. In this work a variable attenuator circuit was constructed to control the tip signal of an active coronary artery catheter in real-time from within the MR scanner room. Performance of the attenuator circuit and the active catheter was characterized on the test bench, in a phantom model, and in vivo. The system was used in a pig model at 3T during the introduction of the catheter into the left coronary artery. The circuit could attenuate the amplitude of the tracking coil signal by up to 20 dB. Without attenuation, the tracking coil signal intensity was masking anatomical details of the coronary ostium making it impossible to reliably introduce the catheter into the artery. After interactive adjustment, which was performed in a few seconds by the interventionalist, the improved visualization of the vascular anatomy enabled a rapid insertion of the catheter into the coronary ostium. The vendor-independent variable attenuator provides real-time control of the catheter signal without interrupting the image acquisition. Even though most MRI systems can control the individual signal levels from coils by software, the attenuator hardware is advantageous as it can be integrated into any MR-system, and it provides a direct interface for the interventionalist at the magnet.

INDEX TERMS Magnetic resonance imaging, active catheter, active tracking, cardiovascular intervention, interventional MRI, radiofrequency coil, actively visualized guidewires, guiding catheters, real time MRI.

I. INTRODUCTION

Magnetic resonance imaging (MRI) has been used for image guidance in diagnostic and therapeutic interventions including coronary catheterization [1]–[4], electrophysiological therapies [5], hepatic tumor ablation [6], [7] and prostate marker implantation [8]. Currently, intravascular interventions such as catheterization or embolization are typically performed under real-time X-ray image guidance. However, MRI would offer several advantages over existing imaging techniques for interventional guidance : MRI does not use ionizing radiation such as X-ray-based imaging methods, MR images can be acquired in arbitrary slice orientations that can be adapted to the anatomy of the patient, MRI offers different image contrasts to differentiate soft tissues and lesions, and it can be combined with functional imaging techniques such as flow measurements to assess the outcome of the intervention quantitatively.

During these procedures the accurate visualization of the interventional instruments (e.g., catheters or guidewires) is

The associate editor coordinating the review of this manuscript and approving it for publication was Zhen Ren.

crucial for providing real-time feedback on the position and orientation of the device [9], [10]. In MRI, passive markers with well-defined susceptibility artifacts [11] have been used for position detection, or inductively coupled RF resonators [12], which enhance the receive sensitivity in their vicinity.

Alternatively, active receive radio frequency (RF) coils or antennas can be attached to the interventional devices for visualization and tracking, that are connected to the MRI receive system via coaxial transmission lines and an interface circuit. Active tracking provides a more robust position detection than passive markers, as the strong positive coil signal is better visible in the images than the marker artifacts. It is also advantageous over inductively coupled coils as the signal is independent of the coupling with the receive coils which can vary during imaging. Depending on the application, a variety of active coil geometries have been used such as regular loop or solenoid coils [13]–[15], loopless antenna designs [16] or dedicated imaging geometries like forward looking coils [17]. Commonly, the coils are remotely tuned and matched in the interface with an additional circuitry for active detuning, for example, by PIN diodes or field effect transistors [18]–[28], and a current trap is added to minimize currents that could lead to unwanted device heating [29]. Tracking catheters without a tuning and matching network have also been reported [30]. It has been shown by several active tracking and imaging coil designs [16], [31]–[33], that tuning and/or matching directly at the coil output is also possible. With recent advances in microstructure production, more components could be embedded on the interventional device, such as low profile capacitors [34], [35]. Interface circuits with impedance control have also been demonstrated to reduce RF-induced heating of various interventional active devices [21], [22], [36]. As an alternative, the RF signal can also be detected after acousto-optic [37] or electro-optic [38] conversion.

During the intervention both conventional imaging coils and tracking coils are used for real-time imaging. The MR signal from the imaging coils provides the anatomical information which is combined with that of the tracking coils – for better visualization this signal can be overlayed in color on the anatomy. The active device coils or antennas are often smaller than the external imaging coils and provide hyper-intense MR signal in the close vicinity. This signal can vary by up to an order of magnitude depending on the orientation of the coil. Thus, during image combination the signals from the active coils are often either too high making it difficult to identify adjacent anatomical features, or they are so low that the device is not clearly detectable in the combined image, as shown in Figure 1.

Dedicated interactive graphical control softwares for real-time imaging allow to modify imaging parameters during the procedure without stopping the imaging protocol [39]–[42]. Real-time control of slice geometry, magnetization preparation, acceleration factors and windowing of reconstructed images has been implemented by several vendors, and systems to allow the interventionalist to control some of these parameters from the magnet room have also been developed. Direct control of the catheter signal independent from the anatomical signal can provide better visual guidance. Besides, it is more practical for the operator to directly control the signal from the active catheter rather than communicating with the control room to adjust the tip signal brightness by repetitive instructions. Although possible in principle, a control system is not yet available for adjusting the signal levels of the active tracking coils from inside the MR room during MRI-guided interventions.

To overcome this limitation, we propose a dedicated interface circuit to manually attenuate the signal intensity of the active coil during the interventional procedure. With this attenuator the interventionalist controls the brightness of the active tracking coil on the MR image interactively at all stages of the intervention. A vendor- and device-independent attenuator was constructed and combined with an active coronary catheter, and the performance of the control circuit was evaluated in a phantom model and a coronary intervention in an animal model at 3 T.

II. METHODS

A. ACTIVE TEST CATHETER DESIGN

For the experiments with the attenuation circuit, an active catheter was used that was made from a commercial 5F guiding catheter (Terumo, Terumo Europe E.V., Leuven, Belgium). A loop coil (4 mm $\times$ 20 mm) was etched from 35 μm copper on a 50 μm polyimide (Kapton^{TM}) substrate and attached to the catheter tip (the coil conductor was 2 mm away from the distal end of the catheter tip) in saddle form resulting in an outer diameter of 5.5 F at the tip together with the isolating polyester heat-shrink tubing (103-0900, Nordson Medical, MA) with 6.4 μm wall-thickness that covers the whole catheter. For signal readout, a 450-μm-outer-diameter coaxial cable (Picocoax PCX40C05; Axon' Kabel GmbH, Leonberg, Germany) was connected to the tracking coil which was integrated into the catheter's inner lumen. The cable had a length of $3\lambda/4 = 155$ cm, and it was connected distally to a tune/match circuit via a bazooka BALUN and a current trap for suppressing common-mode currents. A variable attenuator unit was placed after the tune/match circuit. At the output of the attenuator, another current trap was used. The output signal was then routed to one receive channel of a clinical 3T MRI system (Magnetom PRISMA Fit, Siemens Healthcare, Erlangen) via a *Flex Interface* (Stark Contrast, Erlangen, Germany) that equips a vendor-supplied low noise amplifier with a noise figure of 0.45 and a gain of 29 dB at 123.2 MHz. An overview of the system is shown in Fig. 2.

B. VOLTAGE CONTROLLED ATTENUATOR DESIGN

A PIN diode-based variable attenuator circuit was designed using Pathwave Advanced Design System (ADS 2016, Keysight Technologies, Santa Rosa, CA) to provide an

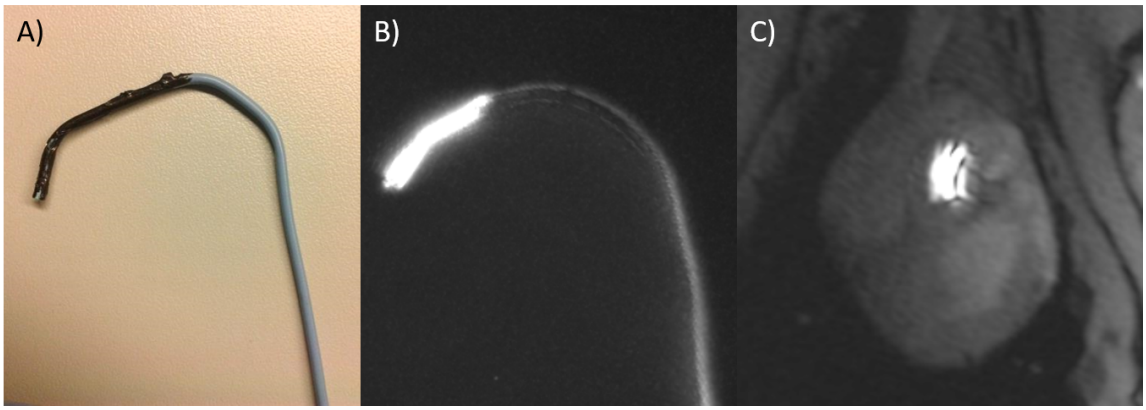

FIGURE 1. Photograph of the 5F active catheter with a saddle coil attached at the tip (A), and high-resolution MR image in a phantom with activated coil (B). MR image with the combined signal from imaging coils and the catheter coil (C). The bright tip coil signal obscures anatomical detail which renders the localization of the catheter tip and visualization of the coronary ostium difficult during an MR-guided coronary intervention. See Methods section for the details of the experimental setup and pulse sequences.

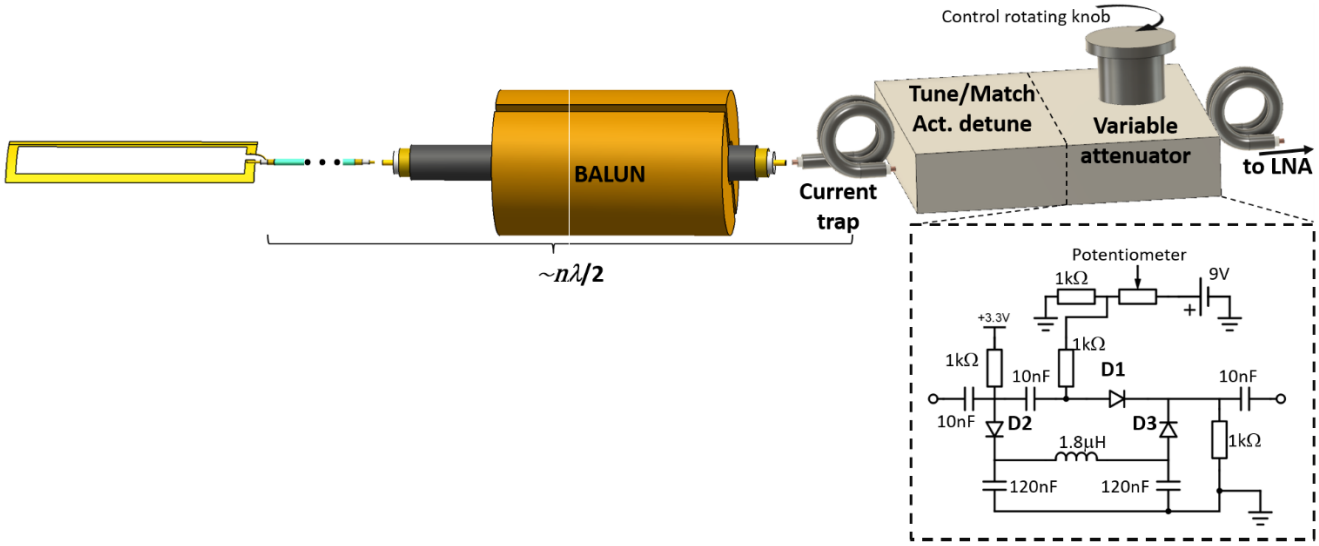

FIGURE 2. Active catheter for visual profiling during real-time MRI and a simplified schematic of the PIN-diode-based variable attenuator circuit. As the voltage across D1 increases, resistance in the RF path will decrease, so as the attenuation level. When D2 and D3 are forward biased, a low resistance RF path towards the ground is created and the tip coil signal will be effectively attenuated. Voltage across D1 is supplied by a 9V nonmagnetic Li-ion battery and controlled with a 10 kΩ potentiometer and a 1 kΩ fixed resistor using a rotating knob and a push-button-switch.

attenuation of the MR signal up to 20 dB, which was inserted between tune/match unit and the MR receiver. In Fig. 2, the placement of the attenuator unit in the receive signal chain of the active catheter is shown. In general, operator-controlled attenuation of the RF signal from the tracking coil can be realized by a resistor network, however, it is well-known that resistance along the MR signal line amplifies the image noise. Besides, PIN-diode based voltage-controlled attenuators are cheap and can be integrated to the tune/match interface easily without adding complexity to the interventional setup unlike connectorized switching attenuator units. Here, a $\pi-$network RF attenuator was realized by using three PIN diodes, D1-3 (MA4P7446F-1091, MACOM, Lowell, CA) that behave as forward-current-controlled resistors. As the forward voltage across D1 decreases, the resistance in the RF path will increase, thus the tip coil signal will be attenuated. An inductor together with two shunt capacitors are included to prevent signal leakage from D1 to D3 that would impair the performance of the circuit (Fig. 2 – dashed box). A non-magnetic 9-V-battery was integrated as the voltage source together with a 10 kΩ potentiometer with rotating knob and a push-button-switch. Potentiometers might exhibit mechanical discontinuities at maximum and minimum rotations. To avoid this, a 3.3V fixed battery shifted the operating point of the attenuator. Depending on the potentiometer and the desired operating point, this feed point can be left floating.

C. MRI MEASUREMENTS

To test the effect of the attenuator on the MR images, a rectangular phantom of $300 \times 400 \times 150$ mm^3 dimensions was filled

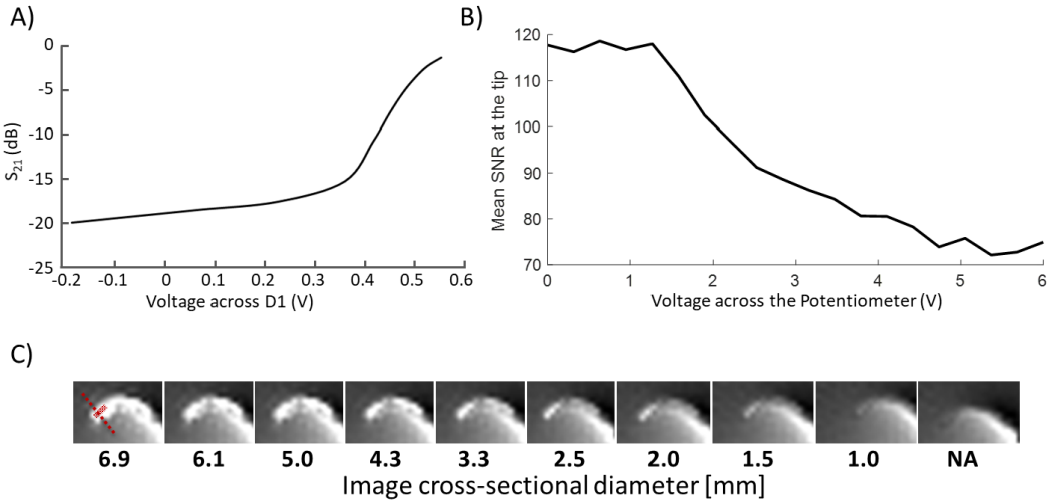

FIGURE 3. A) Test bench measurements of the transmission parameters (S21) using a network analyzer. B) Catheter tip brightness for all the attenuation range was calculated as the mean SNR of the red-marked rectangular region in Fig. 3C. C) Image series for increasing attenuation. The exact shape and the orientation of the tip is closer to the actual dimensions at the optimal attenuation setting.

with 3g/L NaCl and 1g/L CuSO4 solution, and the catheter was immersed with the saddle coil orthogonal to B_0. A real-time imaging sequence (radial-bSSFP: TR = 3.4 ms; TE = 1.5 ms; FOV: 280 × 280 mm^2; base resolution: 160 × 160; radial spokes: 91; slice thickness: 10 mm; flip angle $\alpha = 42°$; bandwidth: 1260 Hz/px) was used to acquire MR images over the available attenuation range. First, the tip profile was measured in mm as the distance between two pixels with 67% of the peak SNR value along the line crosses the tip as highlighted in Fig. 3. SNR was calculated according to [43] from single channel magnitude images acquired solely with the active catheter for the marked rectangular ROIs (Fig. 3) at the tip of the catheter and a signal- and artefact-free region.

In-vivo data was acquired during the animal study described in a previous clinical study [3]: Using the same sequence above ($\alpha = 42°$; bandwidth: 1115 Hz/px, fat saturation), the catheter was introduced through a femoral access and navigated along the aorta to the left coronary artery. To verify the successful engagement of the left coronary artery in the animal experiment, the real-time sequence was again acquired at a higher SNR which was achieved via late-diastolic ECG gating and increasing the number of radial spokes to 181. In addition, a 1% gadolinium solution was injected through the catheter for localized perfusion imaging in a mid-ventricular short-axis view (ECG-gated FLASH: TR = 2.3 ms; TE = 1.1 ms; FOV: 160 × 160 mm^2; base resolution: 160 × 160; slice thickness: 8 mm; $\alpha = 8°$; R = 2; bandwidth: 660 Hz/px, saturation recovery with 123 ms delay). All in-vivo images were acquired with standard posterior 32-channel spine matrix and an anterior 18-channel body array. All experiments were approved by the local ethics committee of Freiburg University and the regional council of Freiburg, Baden-Wuerttemberg, Germany. Experiments were conducted in accordance with FELASA, GV-SOLAS guidelines for animal welfare and reported in accordance with ARRIVE guidelines (see Supplementary Material for details of the animal experiments). In total, the attenuator circuit was used in 20 animal experiments.

D. MRI MEASUREMENTS

The influence of the attenuator on the heating of the catheter was investigated using an ASTM phantom prepared with 30L of Hydroxyethylcellulose gel as described in [44]. Two fibre-optic temperature probes (FOTEMP-19, Weidmann Group, Dresden, Germany) with a thermal resolution of 0.1 C, were fixed to the catheter: One at the most distal point of the tip coil and one at the connection of the coaxial cable to the coil. The catheter was placed 17 cm off center (5 cm from the phantom wall) parallel to B_0 and the phantom wall, with the most distal 58 cm submerged in the gel. This exhibited the largest heating in the presented configuration. The temperature was recorded at 1 s intervals using a service sequence with only RF pulses (2 ms pulse duration, rectangular pulse shape, $\alpha = 188°$, TR = 10ms, reported whole body SAR = 4 W/kg) over a period of 5 min. Cool-down was recorded for another minute. In between measurements, the gel was allowed to cool down until the temperature stabilized to 0.1 C difference in 2 min. 6 attenuation settings were tested covering the range of the possible attenuations. The temperature was measured in two additional scenarios: With the attenuator turned off (no voltage applied across the potentiometer, but still connected to the catheter) and the coil deselected in the scanner's UI.

III. RESULTS

The attenuator circuit had input and output reflection coefficients of $S_{11} = -24.2$dB/ $-$ 8.9dB and $S_{22} = -15.8$dB/ $-$ 11.7dB at minimum/maximum attenuation settings, respectively. In Fig. 3A, transmission

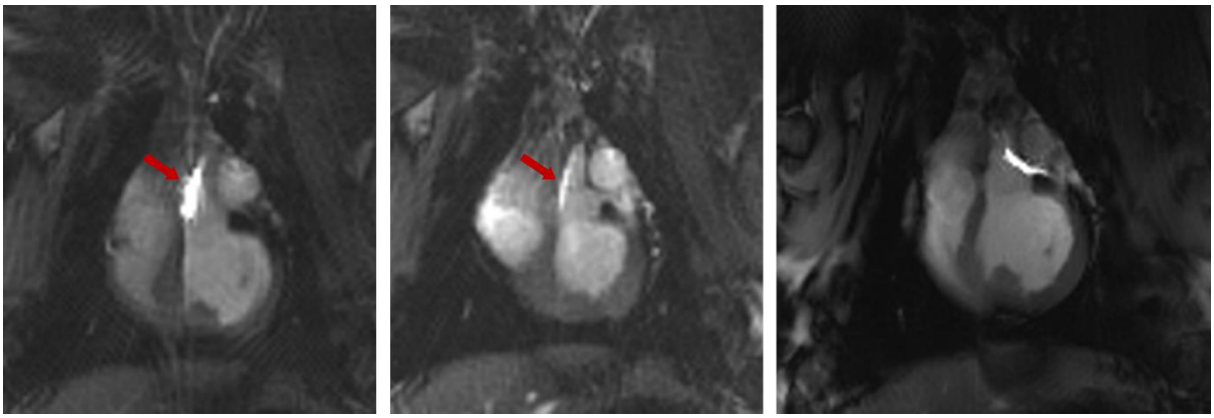

FIGURE 4. Tip brightness monitored via real-time (3 frames/s)bSSFP images as the catheter is navigated across the ascending aorta (left and center). The hyperintense signal of the catheter (left) was attenuated during real-time imaging for optimal contrast (center). With reduced tip signal brightness the catheter was introduced into the left coronary ostium (right, ECG-gated FLASH).

coefficient, S_{12}, across the interface circuit is shown for a range of voltage levels across the series diode, D1, corresponding to the available range of the potentiometer. The circuit covers an attenuation range from -1.7dB to -19.9 dB, and it draws a maximum current of 8 mA, corresponding to a life-time of 150 hours in maximal usage. A photo of the finished circuit can be found in Supporting Information Fig.S1.

In Fig. 3B, the SNR at the tip of the catheter in the phantom experiment is plotted as a function of the voltage across the potentiometer. SNR as a functíon of the voltage across D1 is shown in Supporting Information Fig. S3. Here, the SNR of a manually selected region of interest (ROI) at the tip is given (Fig. 3C). SNR of a regions far away from the tip coil was independent of the attenuation level (SNR $= 61 \pm 3$). Thus, we assume that the image noise is not affected by the attenuator.

Fig. 4 shows real-time images from the coronary artery intervention in a pig. A long axis slice through the descending aorta including the left coronary ostium was chosen to navigate the catheter. Without brightness adjustment, the tip coil intensity is too high, masking anatomical detail and creating streak artifacts. After signal adjustment during real-time imaging the catheter tip could be clearly visualized showing homogeneous contrast. Fully reducing the signal intensity enabled an improved visualization of the anatomical details at the coronary artery (Supporting Information Videos S1, S2). Optimal attenuation settings for the visualization of the tip profile could be found within a few image frames. – In all 24 animal measurements performed using the catheters interfaced with attenuator unit, the catheter could be successfully introduced into the left coronary artery. The average time needed for the navigation of the catheter was 94 ± 37 s including adjustment of the tip signal level, which was necessary after advancing through the proximal ascending aorta to engage the left coronary artery. In most cases one signal adjustment per intervention was sufficient (see Supporting Information Videos S1, S2). In cases where the slice was shifted, the tip signal was re-adjusted. A significant change in the signal profile depending on the orientation of the catheter tip was not observed during the in vivo measurements.

Temperature measurements revealed no dependence of heating on the setting of the attenuator. The temperature was stable for all tested cases with $\Delta T_{max} = 6.4 \pm 0.4$°C for the hotspot at the tip and a $\Delta T_{max} = 3.2 \pm 0.4$°C at the connection to the coax. Background heating was measured to be a $\Delta T_{max} = 0.3 \pm 0.1$°C. Details can be found in Supporting Information Fig. S4. The input impedance of the interface circuit measured from the catheter side was measured as $13.5 \pm 3.1 - j13.8 \pm 4.3\ \Omega$ for the whole attenuation range.

IV. DISCUSSION

In this work, an Rx coil interface circuit with attenuator unit was presented to control the signal intensity of a tracking coil at the tip of a catheter. The attenuator circuit requires a DC power supply to adjust the resistances of PIN diodes in a π-network, which was realized by a battery, but could also be provided by the MRI system. The variable attenuator enabled real-time control of the catheter signal without interrupting the image acquisition which can be crucial in situations where the bright tip signal masks the anatomical target structures.

We preferred PIN-diode-based RF attenuation over resistive attenuators to avoid noise amplification along the signal line. Attenuators in chip form are also commercially available, which can be integrated to an interface circuit for the active devices as shown in Supporting Information Fig. S2, as an example. The PIN diode-based attenuators are usually broadband. The same circuit can also be adapted for active device interface units developed for 1.5 T or any other field strengths. Alternatively, resistive attenuation techniques can also be applied in certain cases, such as rotary step attenuators, which are also commercially available. These devices are however costly and bulky units that can be attached to the receive line via connectors. When such components are

used as an addition to the interface circuit, an alternative DC path needs to be constructed, since, in most MRI systems DC signal for active detuning is carried along the RF receive line. The technique proposed in this paper, however, only modifies the existing interface circuit, i.e., tuning and matching network. Note also that, preamplifiers in MRI receivers have low input impedance. This might cause resistive attenuator networks to raise the noise factor higher than expected. Moreover, MR compatibility of such components needs to be verified. For multi-channel interventional devices, each coil can be controlled separately, or through a single voltage control unit.

In most commercial MRI systems, the active detuning signal that is activated in Rx coils during Tx is supplied through the receive line, i.e., RF path. It is also possible to control the attenuator using the voltage supplied by the MRI system to eliminate the battery usage. With the system-supplied DC signal, there is no need for a battery exchange or charging, the interface circuit is lighter, smaller, and mechanically less complicated. However, since the voltage-controlled attenuator is active during Rx but the detuning signal is active during Tx, it is not possible to share the same source. Alternatively, the DC signal from a second Rx channel or any other system-supplied source can be coupled to the active catheter to control the attenuator. Since the MRI system allows control of the timings of DC signals independently, attenuator and detuning functions can run without interfering.

MRI systems can control the signal levels from the individual receive coils by software so that the adjustment of the tip coil brightness could also be realized during image reconstruction using an interactive input from a user interface. However, the proposed hardware solution is advantageous as it is system- and vendor-independent so that it can be used with any MR-system, and the existing reconstruction and coil combination software does not need to be modified. Furthermore, it provides a direct, tangible interface for the interventionalist at the distal end of the catheter. This construction makes it very simple to use even during cardiac interventions where the interventionalist needs to have optimal control and rapid feedback without complicated user interface interactions.

Note, that the metal braided catheter used in this study is not MR safe according to the temperature measurements. However, as mentioned in the previous paragraph, the attenuator approach we presented in this paper can be combined with or applied to any active devices including active catheters, actively visualized guidewires, or biopsy needles. RF-induced heating can be influenced by the distal impedance [21] – thus, the heating of an active device might change with the attenuation level if the input impedance of the attenuator circuit is dependent on the resistance of the PIN diodes. In most of the cases, active devices are used for visual profiling during MRI-guided interventions and they introduced to the MRI system as receive-only RF coils. Thus, they are detuned during the Tx cycle using a PIN diode as shown in Supporting Information Fig. S2. During the Tx cycle, PIN diode is switched ON, and the impedance seen from the coil side is dominated by the detuning elements, and is not affected from the attenuator. For the interface circuit used in this study, the input impedance for the whole attenuation range was measured as $13.5 \pm 3.1 - j13.8 \pm 4.3\ \Omega$. Therefore a significant dependence of the RF-induced heating on the attenuation level is not expected. Temperature measurements confirm also that, the attenuator did not have any measureable effect on the RF-induced heating of the catheter. The attenuator can also be combined with an impedance control unit [22] in a switchable way (i.e., the attenuator is active during Rx and impedance control is active during Tx to reduce RF-induced heating). Alternatively, both input and output-matched attenuators, such as hybrid coupler based attenuators, can be used that keep the input and output impedances fixed at all attenuation levels [45]. Note, also that the attenuator unit doesn't impose any risks due to the DC current on the patient as the DC currents are blocked by the tuning and matching capacitors already at the interface circuit.

Another use of the attenuator circuit is the detection of catheters that are near, but not in, the imaging slice: if the signal from the tip is maximized, the faint stray sensitivity of the tip coil can be sufficient to see it even when the catheter has left the image plane depending on the distance between the tracking coil and the imaging plane, and the coil geometry. This can also be achieved by an analog operator-controlled preamplifier stage similar to the attenuator. Although, the image SNR cannot be increased, when the relative gain of the active catheter's receive channel increases, tip signal will be relatively higher than the other channels, which could help recovering the location of the catheter in certain cases. A manual switching between the attenuator and the variable-gain preamplifier can be implemented to allow the operator full flexibility. Another function that can be implemented with manual control is analog multi-coil selection of multiple tracking coils such as in Kocaturk *et al.* [46].

In this work, remote tuning and matching was implemented as it reduced the complexity of the tip coil design. Remote tuning and matching is the most commonly used technique in active tracking coils as it does not compromise size and mechanical stability. We have used a single-turn loop coil in saddle form soldered to a microcoaxial cable, but the voltage-controlled attenuator approach can be applied to other coil and interface circuit combinations.

V. CONCLUSION

An RF-attenuator integrated into the interface circuits of active interventional devices can enable interventionalists to control hyperintense signals in close vicinity of the tip coils that can otherwise mask the anatomy. The proposed design can be a low-cost solution for interventional MRI suits which lack a dedicated real-time signal level adjustment unit for individual Rx channels.

ACKNOWLEDGMENT

The authors thank Dr. Roland Galmbacher, Dr. Heidi Christina Schmitz, and Julien Thielmann for their support during the animal trials. The authors declare that they have no competing interests. The datasets acquired and/or analyzed during the current study are available from the corresponding author on reasonable request. Detailed circuit schematics, PCB designs, and 3-D CAD models of both interface circuits can be found in https://github.com/ozenEEE/ActiveTrackingHardware. *(Ali C. Özen and Thomas Lottner contributed equally to this work.)*

REFERENCES

[1] J.-M. Serfaty, X. Yang, T. K. Foo, A. Kumar, A. Derbyshire, and E. Atalar, "MRI-guided coronary catheterization and PTCA: A feasibility study on a dog model," *Magn. Reson. Med.*, vol. 49, no. 2, pp. 258–263, Feb. 2003, doi: 10.1002/mrm.10393.

[2] R. A. Omary, J. D. Green, B. E. Schirf, Y. Li, J. P. Finn, and D. Li, "Real-time magnetic resonance imaging-guided coronary catheterization in swine," *Circulation*, vol. 107, no. 21, pp. 2656–2659, Jun. 2003, doi: 10.1161/01.CIR.0000074776.88681.F5.

[3] T. Heidt, S. Reiss, A. J. Krafft, A. C. Özen, T. Lottner, C. Hehrlein, R. Galmbacher, G. Kayser, I. Hilgendorf, P. Stachon, D. Wolf, A. Zirlik, K. Düring, M. Zehender, S. Meckel, D. von Elverfeldt, C. Bode, M. Bock, and C. von zur Mühlen, "Real-time magnetic resonance imaging–guided coronary intervention in a porcine model," *Sci. Rep.*, vol. 9, no. 1, p. 8663, Dec. 2019, doi: 10.1038/s41598-019-45154-7.

[4] T. Heidt, S. Reiss, T. Lottner, A. C. Özen, C. Bode, M. Bock, and C. von zur Mühlen, "Magnetic resonance imaging for pathobiological assessment and interventional treatment of the coronary arteries," *Eur. Heart J. Supplements*, vol. 22, pp. C46–C56, Apr. 2020, doi: 10.1093/eurheartj/suaa009.

[5] M. Gutberlet, M. Grothoff, C. Eitel, C. Lücke, P. Sommer, C. Piorkowski, and G. Hindricks, "First clinical experience in man with the IMRICOR-MR-EP system: Electrophysiology study guided by real-time MRI," *J. Cardiovascular Magn. Reson.*, vol. 14, no. S1, p. P205, Dec. 2012, doi: 10.1186/1532-429X-14-S1-P205.

[6] J. A. Bell, C. E. Saikus, K. Ratnayaka, V. Wu, M. Sonmez, A. Z. Faranesh, J. H. Colyer, R. J. Lederman, and O. Kocaturk, "A deflectable guiding catheter for real-time MRI-guided interventions," *J. Magn. Reson. Imag.*, vol. 35, no. 4, pp. 908–915, Apr. 2012, doi: 10.1002/jmri.23520.

[7] R. Hoffmann, H. Rempp, D.-E. Keßler, J. Weiß, P. L. Pereira, K. Nikolaou, and S. Clasen, "MR-guided microwave ablation in hepatic tumours: Initial results in clinical routine," *Eur. Radiol.*, vol. 27, pp. 1467–1476, Apr. 2017, doi: 10.1007/s00330-016-4517-x.

[8] A. Krieger, R. C. Susil, C. Ménard, J. A. Coleman, G. Fichtinger, E. Atalar, and L. L. Whitcomb, "Design of a novel MRI compatible manipulator for image guided prostate interventions," *IEEE Trans. Biomed. Eng.*, vol. 52, no. 2, pp. 306–313, Feb. 2005, doi: 10.1109/TBME.2004.840497.

[9] M. Bock and F. K. Wacker, "MR-guided intravascular interventions: Techniques and applications," *J. Magn. Reson. Imag.*, vol. 27, no. 2, pp. 326–338, Feb. 2008, doi: 10.1002/jmri.21271.

[10] M. Bock, S. Müller, S. Zuehlsdorff, P. Speier, C. Fink, P. Hallscheidt, R. Umathum, and W. Semmler, "Active catheter tracking using parallel MRI and real-time image reconstruction," *Magn. Reson. Med.*, vol. 55, no. 6, pp. 1454–1459, Jun. 2006, doi: 10.1002/mrm.20902.

[11] A. Massmann, A. Buecker, and G. K. Schneider, "Glass-fiber–based MR-safe guidewire for MR imaging–guided endovascular interventions: *in vitro* and preclinical *in vivo* feasibility study," *Radiology*, vol. 284, no. 2, pp. 541–551, Aug. 2017, doi: 10.1148/radiol.2017152742.

[12] H. H. Quick, M. O. Zenge, H. Kuehl, G. Kaiser, S. Aker, S. Massing, S. Bosk, and M. E. Ladd, "Interventional magnetic resonance angiography with, no., strings attached: Wireless active catheter visualization," *Magn. Reson. Med.*, vol. 53, no. 2, pp. 446–455, Feb. 2005, doi: 10.1002/mrm.20347.

[13] K. Kandarpa, P. Jakab, S. Patz, F. J. Schoen, and F. A. Jolesz, "Prototype miniature endoluminal MR imaging catheter," *J. Vascular Interventional Radiol.*, vol. 4, no. 3, pp. 419–427, May 1993, doi: 10.1016/S1051-0443(93)71891-6.

[14] G. C. Hurst, J. Hua, J. L. Duerk, and A. M. Cohen, "Intravascular (catheter) NMR receiver probe: Preliminary design analysis and application to canine iliofemoral imaging," *Magn. Reson. Med.*, vol. 24, no. 2, pp. 343–357, Apr. 1992, doi: 10.1002/mrm.1910240215.

[15] A. J. Martin, D. B. Plewes, and R. M. Henkelman, "MR imaging of blood vessels with an intravascular coil," *J. Magn. Reson. Imag.*, vol. 2, no. 4, pp. 421–429, Jul. 1992, doi: 10.1002/jmri.1880020411.

[16] O. Ocali and E. Atalar, "Intravascular magnetic resonance imaging using a loopless catheter antenna," *Magn. Reson. Med.*, vol. 37, no. 1, pp. 112–118, Jan. 1997, doi: 10.1002/mrm.1910370116.

[17] K. J. T. Anderson, G. Leung, A. J. Dick, and G. A. Wright, "Forward-looking intravascular orthogonal-solenoid coil for imaging and guidance in occlusive arterial disease," *Magn. Reson. Med.*, vol. 60, no. 2, pp. 489–495, Aug. 2008, doi: 10.1002/mrm.21667.

[18] W. Wang, C. L. Dumoulin, A. N. Viswanathan, Z. T. H. Tse, A. Mehrtash, W. Loew, I. Norton, J. Tokuda, R. T. Seethamraju, T. Kapur, A. L. Damato, R. A. Cormack, and E. J. Schmidt, "Real-time active MR-tracking of metallic stylets in MR-guided radiation therapy," *Magn. Reson. Med.*, vol. 73, no. 5, pp. 1803–1811, May 2015, doi: 10.1002/mrm.25300.

[19] C. Fink, M. Bock, R. Umathum, S. Volz, S. Zuehlsdorff, R. Grobholz, H.-U. Kauczor, and P. Hallscheidt, "Renal embolization: Feasibility of magnetic resonance-guidance using active catheter tracking and intraarterial magnetic resonance angiography," *Investigative Radiol.*, vol. 39, no. 2, pp. 111–119, Feb. 2004, doi: 10.1097/01.rli.0000110744.70512.df.

[20] G. G. Zimmermann-Paul, M. E. Ladd, T. Pfammatter, P. R. Hilfiker, H. H. Quick, and J. F. Debatin, "MR versus fluoroscopic guidance of a catheter/guidewire system: *in vitro* comparison of steerability," *J. Magn. Reson. Imag.*, vol. 8, no. 5, pp. 1177–1181, Sep. 1998, doi: 10.1002/jmri.1880080526.

[21] A. C. Özen, T. Lottner, and M. Bock, "Safety of active catheters in MRI: Termination impedance versus RF-induced heating," *Magn. Reson. Med.*, vol. 81, no. 2, pp. 1412–1423, Feb. 2019, doi: 10.1002/mrm.27481.

[22] A. C. Özen, B. Silemek, T. Lottner, E. Atalar, and M. Bock, "MR safety watchdog for active catheters: Wireless impedance control with real-time feedback," *Magn. Reson. Med.*, vol. 84, no. 2, pp. 1048–1060, Aug. 2020, doi: 10.1002/mrm.28153.

[23] O. Kocaturk, A. H. Kim, C. E. Saikus, M. A. Guttman, A. Z. Faranesh, C. Ozturk, and R. J. Lederman, "Active two-channel 0.035" guidewire for interventional cardiovascular MRI," *J. Magn. Reson. Imag.*, vol. 30, no. 2, pp. 461–465, Aug. 2009, doi: 10.1002/jmri.21844.

[24] S. Fandrey, S. Weiss, and J. Müller, "A novel active MR probe using a miniaturized optical link for a 1.5-T MRI scanner," *Magn. Reson. Med.*, vol. 67, no. 1, pp. 148–155, Jan. 2012, doi: 10.1002/mrm.23002.

[25] A. Alipour, E. S. Meyer, C. L. Dumoulin, R. D. Watkins, H. Elahi, W. Loew, J. Schweitzer, G. Olson, Y. Chen, S. Tao, M. Guttman, A. Kolandaivelu, H. R. Halperin, and E. J. Schmidt, "MRI conditional actively tracked metallic electrophysiology catheters and guidewires with miniature tethered radio-frequency traps: Theory, design, and validation," *IEEE Trans. Biomed. Eng.*, vol. 67, no. 6, pp. 1616–1627, Jun. 2020, doi: 10.1109/TBME.2019.2941460.

[26] J. G. Miller, M. Li, D. Mazilu, T. Hunt, and K. A. Horvath, "Real-time magnetic resonance imaging–guided transcatheter aortic valve replacement," *J. Thoracic Cardiovascular Surgery*, vol. 151, no. 5, pp. 1269–1277, May 2016, doi: 10.1016/j.jtcvs.2015.11.024.

[27] L. Feng, C. L. Dumoulin, S. Dashnaw, R. D. Darrow, R. Guhde, R. L. DeLaPaz, P. L. Bishop, and J. Pile-Spellman, "Transfemoral catheterization of carotid arteries with real-time MR imaging guidance in pigs," *Radiology*, vol. 234, no. 2, pp. 551–557, Feb. 2005, doi: 10.1148/radiol.2341031951.

[28] M. E. Ladd, G. G. Zimmermann, G. C. McKinnon, G. K. von Schulthess, C. L. Dumoulin, R. D. Darrow, E. Hofmann, and J. F. Debatin, "Visualization of vascular guidewires using MR tracking," *J. Magn. Reson. Imag.*, vol. 8, no. 1, pp. 251–253, Jan. 1998, doi: 10.1002/jmri.1880080142.

[29] P. V. Karmarkar, D. L. Kraitchman, I. Izbudak, L. V. Hofmann, L. C. Amado, D. Fritzges, R. Young, M. Pittenger, J. W. M. Bulte, and E. Atalar, "MR-trackable intramyocardial injection catheter," *Magn. Reson. Med.*, vol. 51, no. 6, pp. 1163–1172, Jun. 2004, doi: 10.1002/mrm.20086.

[30] B. R. Daniels, R. Pratt, R. Giaquinto, and C. Dumoulin, "Optimizing accuracy and precision of micro-coil localization in active-MR tracking," *Magn. Reson. Imag.*, vol. 34, no. 3, pp. 289–297, Apr. 2016, doi: 10.1016/j.mri.2015.11.005.

[31] C. M. Hillenbrand, D. R. Elgort, E. Y. Wong, A. Reykowski, F. K. Wacker, J. S. Lewin, and J. L. Duerk, "Active device tracking and high-resolution intravascular MRI using a novel catheter-based, opposed-solenoid phased array coil," *Magn. Reson. Med.*, vol. 51, no. 4, pp. 668–675, Apr. 2004, doi: 10.1002/mrm.20050.

[32] F. K. Wacker, D. Elgort, C. M. Hillenbrand, J. L. Duerk, and J. S. Lewin, "The catheter-driven MRI scanner: A new approach to intravascular catheter tracking and imaging-parameter adjustment for interventional MRI," *Amer. J. Roentgenol.*, vol. 183, no. 2, pp. 391–395, Aug. 2004, doi: 10.2214/ajr.183.2.1830391.

[33] E. J. Schmidt, G. Olson, J. Tokuda, A. Alipour, R. D. Watkins, E. M. Meyer, and H. Elahi, "Intracardiac MR imaging (ICMRI) guiding-sheath with amplified expandable-tip imaging and MR-tracking for navigation and arrythmia ablation monitoring: Swine testing at 1.5 and 3T," *Magn. Reson. Med.*, pp. 1–16, Feb. 2022, doi: 10.1002/mrm.29168.

[34] E. Baysoy, D. K. Yildirim, C. Ozsoy, S. Mutlu, and O. Kocaturk, "Thin film based semi-active resonant marker design for low profile interventional cardiovascular MRI devices," *Magn. Reson. Mater. Phys., Biol. Med.*, vol. 30, no. 1, pp. 93–101, Feb. 2017, doi: 10.1007/s10334-016-0586-8.

[35] O. Nassar, D. Mager, and J. G. Korvink, "A novel sensor design and fabrication for wireless interventional MRI through induction coupling," in *Proc. IEEE SENSORS*, Oct. 2019, pp. 1–4, doi: 10.1109/SENSORS43011.2019.8956525.

[36] V. Acikel, B. Silemek, and E. Atalar, "Wireless control of induced radiofrequency currents in active implantable medical devices during MRI," *Magn. Reson. Med.*, vol. 83, no. 6, pp. 2370–2381, Jun. 2020, doi: 10.1002/mrm.28089.

[37] Y. S. Yaras, D. K. Yildirim, D. A. Herzka, T. Rogers, A. E. Campbell-Washburn, R. J. Lederman, F. L. Degertekin, and O. Kocaturk, "Real-time device tracking under MRI using an acousto-optic active marker," *Magn. Reson. Med.*, vol. 85, no. 5, pp. 2904–2914, May 2021, doi: 10.1002/mrm.28625.

[38] R. C. Susil, C. J. Yeung, H. R. Halperin, A. C. Lardo, and E. Atalar, "Multifunctional interventional devices for MRI: A combined electrophysiology/MRI catheter," *Magn. Reson. Med.*, vol. 47, no. 3, pp. 594–600, Mar. 2002, doi: 10.1002/mrm.10088.

[39] M. Bock, S. Volz, S. Zühlsdorff, R. Umathum, C. Fink, P. Hallscheidt, and W. Semmler, "MR-guided intravascular procedures: Real-time parameter control and automated slice positioning with active tracking coils," *J. Magn. Reson. Imag.*, vol. 19, no. 5, pp. 580–589, May 2004, doi: 10.1002/jmri.20044.

[40] M. A. Guttman, C. Ozturk, A. N. Raval, V. K. Raman, A. J. Dick, R. DeSilva, P. Karmarkar, R. J. Lederman, and E. R. McVeigh, "Interventional cardiovascular procedures guided by real-time MR imaging: An interactive interface using multiple slices, adaptive projection modes and live 3D renderings," *J. Magn. Reson. Imag.*, vol. 26, no. 6, pp. 1429–1435, Dec. 2007, doi: 10.1002/jmri.21199.

[41] S. R. Yutzy and J. L. Duerk, "Pulse sequences and system interfaces for interventional and real-time MRI," *J. Magn. Reson. Imag.*, vol. 27, no. 2, pp. 267–275, Feb. 2008, doi: 10.1002/jmri.21268.

[42] A. E. Campbell-Washburn, A. Z. Faranesh, R. J. Lederman, and M. S. Hansen, "Magnetic resonance sequences and rapid acquisition for MR-guided interventions," *Magn. Reson. Imag. Clinics North Amer.*, vol. 23, no. 4, pp. 669–679, Nov. 2015, doi: 10.1016/j.mric.2015.05.006.

[43] R. M. Henkelman, "Measurement of signal intensities in the presence of noise in MR images," *Med. Phys.*, vol. 12, no. 2, pp. 232–233, 1985, doi: 10.1118/1.595711.

[44] "Designation: ASTM F2182-11a, standard test method for measurement of radio frequency induced heating near passive implants during magnetic resonance imaging," Amer. Soc. Test. Mater. Int., West Conshohocken, PA, USA, Tech. Rep., 2011, p. 12, doi: 10.1520/F2182-11.

[45] A. C. Özen, E. Atalar, J. G. Korvink, and M. Bock, "*In vivo* MRI with concurrent excitation and acquisition using automated active analog cancellation," *Sci. Rep.*, vol. 8, no. 1, p. 10631, Dec. 2018, doi: 10.1038/s41598-018-28894-w.

[46] O. Kocaturk, C. E. Saikus, M. A. Guttman, A. Z. Faranesh, K. Ratnayaka, C. Ozturk, E. R. McVeigh, and R. J. Lederman, "Whole shaft visibility and mechanical performance for active MR catheters using copper-nitinol braided polymer tubes," *J. Cardiovascular Magn. Reson.*, vol. 11, no. 1, p. 29, Dec. 2009, doi: 10.1186/1532-429X-11-29.

ALI C. ÖZEN (Senior Member, IEEE) was born in Turkey, in 1988. He received the bachelor's degree in electrical and electronics engineering and the master's degree from Bilkent University, Ankara, in 2011 and 2013, respectively, and the Ph.D. degree from the Institute of Microstructure Technology, Karlsruhe Institute of Technology, Germany, in 2017.

In 2013, he joined the Department of Radiology, Medical Physics, University Medical Center Freiburg, as a Research Assistant, where he became a Postdoctoral Fellow, in 2017. From 2017 to 2021, he was a Scientist working with the German Consortium for Translational Cancer Research Partner Site Freiburg. He is currently an Engineer and leading the novel RF coil and electronics development projects with the Medical Physics Department, University Medical Center Freiburg. He is involved in scientific research and technology development in the fields of magnetic resonance imaging, cardiovascular interventions, and MR safety.

Dr. Özen is a member of the International Society of Magnetic Resonance in Medicine and a School of Oncology Fellow of German Cancer Research Center (DKFZ). He was a recipient of the Young Investigator Award of European Society of Magnetic Resonance in Medicine and Biology in 2015. In 2019, he received the Lasby Fellowship from the University of Minnesota. In 2021, he was honored with a Senior Membership by IEEE.

THOMAS LOTTNER (Member, IEEE) was born in Regensburg, Germany, in 1991. He received the bachelor's degree in physics from the University of Regensburg, in 2013, and the master's degree in 2016. He is currently pursuing the Ph.D. degree with the Department of Radiology, Medical Physics, University Medical Center Freiburg, where he is working on magnetic resonance imaging, RF simulations, MR guided interventions, and MR safety.

He is a member of the International Society of Magnetic Resonance in Medicine.

SIMON REISS was born in Freiburg, Germany, in 1989. He received the bachelor's degree in physics from the University of Freiburg, in 2011, and the master's degree in 2014. He is currently pursuing the Ph.D. degree with the Department of Radiology, Medical Physics, University Medical Center Freiburg, where he is working on magnetic resonance imaging, MR-guided interventions, and MR safety.

He is a member of the International Society of Magnetic Resonance in Medicine.

TIMO HEIDT received the Medical degree from the University of Saarland and the University of Freiburg, in 2009, and the Habilitation degree in 2018. In 2020, he received the board certification in internal medicine and cardiology. In 2009, he became a Clinical Fellow with the Internal Medicine Department, University Medical Center Freiburg. From 2011 to 2013, he worked as a Postdoctoral Researcher with the Center for Systems Biology, Massachusetts General Hospital and Harvard Medical School, Boston, MA, USA. In 2019, he was appointed as an Attending Physician with the Department of Cardiology and Angiology I, University Heart Center Freiburg, Bad Krozingen. He has published over 40 articles on the therapy and diagnosis of myocardial diseases. He investigates novel biomarkers to monitor myocardial infarction.

CONSTANTIN VON ZUR MÜHLEN received the Medical degree from the University of Würzburg, Germany, in 2003. He studied medicine in Oxford, U.K.; Cleveland, USA; and Basel, Switzerland, from 1997 to 2003. In 2010, he completed his certification for internal medicine and appointed as an Assistant Professor in cardiology. In 2013, he became the Deputy of the Chairperson in cardiology and the Head of interventional cardiology with the Department of Cardiology and Angiology, University Medical Center Freiburg. He is also the Head of the Cardiovascular Imaging and Immunology Research Group. He has published over 100 articles in interventional cardiology and cardiovascular imaging.

MICHAEL BOCK was born in Helmstedt, Germany, in 1966. He studied at the University of Braunschweig and the University of Heidelberg. He received the Diploma degree in physics from the Max Planck Institute for Nuclear Physics, in 1992, the Ph.D. degree in physics from the German Cancer Research Center (DKFZ), University of Heidelberg, Heidelberg, in 1995, worked on MRI-based velocity measurements, and the Habilitation degree in interventional MRI from the Medical Faculty, Heidelberg University, in 2009.

Since 2011, he has been a Professor for experimental radiology with the University Medical Center Freiburg, Germany. At DKFZ, he has been working since 1996, as a Group Leader focusing on the implementation of technologies and methods for MRI-guided interventions. In 2007, he coordinated the installation of a 7-T research whole body system for ultra-high field MRI in oncology. He held visiting professorships at the University of Prague and the University of Cleveland. He has published more than 200 journal articles, and supervised five bachelor's, 23 master's, and 33 Ph.D. theses. His work focuses on various aspects of MR imaging technologies, including for example fast real-time MRI for interventions, x-nuclear imaging with ^{17}O, and MR imaging protocols for oncology.

Prof. Bock is a member of the International Society for Magnetic Resonance in Medicine (ISMRM) and various physics societies. Among other awards, he received the Life-Time Science Award from the German Society for Medical Physics (DGMP) in 2010.